Published in final edited form as:
Angew Chem Int Ed Engl. 2016 March 1; 55(10): 3309–3312. doi:10.1002/anie.201509183.

Polymeric Nanoparticles Amenable to Simultaneous Installation of Exterior Targeting and Interior Therapeutic Proteins

Dr. Xi Zhu[a,b], **Dr. Jun Wu**[b], **Wei Shan**[a], **Dr. Wei Tao**[b], **Dr. Lili Zhao**[b], **Dr. Jong-Min Lim**[b,c], **Mr. Mathew D'Ortenzio**[b], **Prof. Rohit Karnik**[c], **Prof. Yuan Huang**[a], **Prof. Jinjun Shi**[b], and **Prof. Omid C. Farokhzad**[b,d]

Yuan Huang: huangyuan0@163.com; Jinjun Shi: jshi@bwh.harvard.edu; Omid C. Farokhzad: ofarokhzad@bwh.harvard.edu

[a]Key Laboratory of Drug Targeting and Drug Delivery System, Ministry of Education, West China School of Pharmacy, Sichuan University, Chengdu 610041(China)

[b]Department of Anesthesiology, Brigham and Women's Hospital, Harvard Medical School, Boston, MA02115 (USA)

[c]Department of Mechanical Engineering, Massachusetts Institute of Technology, Cambridge, MA 02139 (USA)

[d]King Abdulaziz University, Jeddah, Saudi Arabia

Abstract

Effective delivery of therapeutic proteins a formidable challenge. Herein, using a unique polymer family with a wide-ranging set of cationic and hydrophobic features, we developed a novel nanoparticle (NP) platform capable of installing protein ligands on the particle surface and simultaneously carrying therapeutic proteins inside by a self-assembly procedure. The loaded therapeutic proteins (e.g., insulin) within the NPs exhibited sustained and tunable release, while the surface-coated protein ligands (e.g., transferrin) were demonstrated to alter the NP cellular behaviors. In vivo results revealed that the transferrin-coated NPs can effectively be transported across the intestinal epithelium for oral insulin delivery, leading to a notable hypoglycemic response.

Graphical Abstract

Correspondence to: Yuan Huang, `huangyuan0@163.com`; Jinjun Shi, `jshi@bwh.harvard.edu`; Omid C. Farokhzad, `ofarokhzad@bwh.harvard.edu`.

X.Z. and J.W. contributed equally to this work.

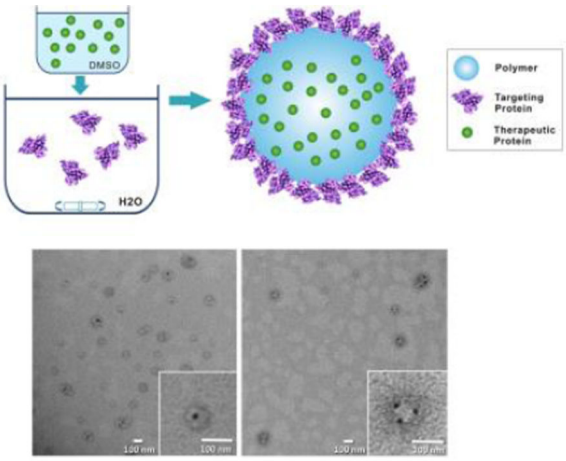

A novel polymeric nanoparticle platform that is capable of installing protein ligands on the particle surface and simultaneously carrying therapeutic proteins inside was developed in a single self-assembly step. The surface coating with transferrin drastically changes the cellular behavior of the nanoparticles and enhances their transepithelial transport via transcytosis. By loading insulin within the transferrin-coated nanoparticles, a notable hypoglycemic response is elicited following oral administration.

Keywords

Protein delivery; Nanoparticle; Insulin; Transcytosis

Protein-based therapies have been increasingly important in the treatment of various diseases since 1970s[1]. However, safe and effective delivery of protein therapeutics to desired disease tissues remains a significant challenge, largely due to unfavorable properties of most proteins[2]. This situation is well exemplified by the barriers posed by the oral administration of protein drugs (e.g. insulin)[3]. Rapid digestive degradation and low permeability through the intestinal epithelium make the oral absorption of insulin highly inefficient.

Numerous NP platforms have been developed for the delivery of proteins[1b, 3a]. However, the capability of these NPs for protein delivery applications remains limited, due to low loading efficiency and uncontrollable release profiles. Ideal protein delivery NP platform should possess at least the following characteristics: effective protein loading and protection; sustainable protein release; and a simple formulation strategy that preserves the bioactivity of proteins. Moreover, NPs for oral delivery have to overcome the transport barrier of the intestinal epithelium. Receptor-mediated transcytosis[4] has exhibited significant potential in promoting transepithelial absorption. For example, neonatal FcRn-mediated transcytosis of NPs that target the FcRn receptor has recently been shown to be a feasible approach for transepithelial transport of therapeutics[5].One important obstacle these NPs still face is that surface modification with protein-based ligands after protein loading should be avoided due to their susceptibility to conjugation reactions and unwanted release.

Here we report development of a novel NP platform that is capable of simultaneous installation of targeting proteins on the exterior and loading of therapeutic proteins in the interior of the NP in a single self-assembly step (Figure 1a). Since major types of proteins are negatively charged, and have hydrophobic regions[2, 6], we hypothesized that polymers with combined cationic and hydrophobic characteristics may have a strong affinity with proteins. Therefore, we developed a family of water-insoluble polymers with a wide-ranging, yet tunable, set of cationic and hydrophobic features. These polymers can form NPs *via* simple self-assembly, and therapeutic and targeting proteins can be simultaneously installed interiorly and exteriorly, respectively. The physically loaded targeting proteins on the NP surface were demonstrated to alter the NP's behaviors, and the encapsulated proteins within the NPs were well protected and exhibited sustained and tunable release. To demonstrate feasibility of protein delivery of this NP platform, we explored oral absorption of the NPs for treating diabetes. Insulin was loaded inside the NPs as a therapeutic protein, while transferrin (Tf), a classical protein that can undergo transcytosis by binding to Tf receptors on epithelial cells[7],was installed as a model targeting protein.

We chose poly(ester amide)s (PEAs) as NP material, which are composed of amino acids, diols, and diacids (Figure 1b). Arginine (Arg) was used as the cationic component, and Phenylalanine (Phe) was chosen to mediate intra- and intermolecular interactions *via* hydrophobic force. PEAs were prepared via the solution polycondensation of monomers with various Phe to Arg ratios by changing the feed ratios of monomers I to II (Figure 1b, Table S1)[8]. The synthesis details could be found in Supporting Information (SI) (Figure S1). The five Phe-Arg-PEAs obtained are referred to as PEA10, PEA25, PEA50, PEA75, and PEA90, where the number indicates the molar percent of L-Phe diester monomer in L-Phe and L-Arg diester monomers.

The polymeric NPs were prepared *via* a novel single-step nanoprecipitation method (Figure 1a and SI). To do this, the polymer and insulin were first dissolved in DMSO. When the freshly prepared DMSO solution was added to a rapidly mixing aqueous solution containing targeting Tf proteins, the polymer molecules spontaneously formed a solid NP core encapsulating insulin. Meanwhile, the Tf proteins in the aqueous solution were captured onto the NP surface via their affinity with the polymer. As a proof of concept, the NPs were prepared with the five different PEAs aforementioned, or 1:1 wt% mixture of PEA and poly(lactic-*co*-glycolic acid) (PLGA). The resulting PEA and PLGA-PEA NPs had size of 80–110 nm (Table S2 in SI). Transmission electron microscopy (TEM) images showed that these NPs are spherical and exhibit a core-shell structure with a distinct protein coating (Figure 1c). In comparison, the NPs without a surface protein coating did not exhibit the core-shell structure (Figure 1d). To further clarify the NP structure, bovine serum albumin (BSA) conjugated with gold nanospheres (5 nm) (BSA-Au) were used in the NP formulation. When the BSA-Au was dissolved in DMSO and co-precipitated with the polymer (representing a therapeutic protein), it was completely encapsulated within the NPs (Figure 1e). By contrast, the BSA-Au was loaded on the NP surface when it was dissolved in the aqueous solution, representing a targeting protein (Figure 1f).

Hydrophobicity and charge density of the PEAs can easily be tuned by changing the Phe/Arg ratio, and thus the NPs can also exhibit a broad range of properties. All prepared

NPs possessed surface charges ranging from + 11.8 to + 31.3 mV (Figure 2a and Table S2). The NPs with higher percentages of Arg had a higher zeta potential. Micro-environmental hydrophobicity of the PEA NPs was compared using Coomassie Brilliant Blue G-250 (CBB) as a polarity-sensitive probe[9]. A bathochromic shift (Δλ) of absorption peak of CBB indicates an increase in micro-environmental hydrophobicity. NPs with higher Phe/Arg ratio exhibited larger shifts, suggesting higher hydrophobicity (Figures 2a and S4). We postulated that the NPs with higher Phe/Arg ratios might possess a more compact matrix due to stronger hydrophobic interactions, while those with lower ratios might be less compact due to stronger electrostatic repulsion. The NPs were examined for their encapsulation efficiency (EE) and loading efficiency (LE) of insulin. Among all the PEA NPs, PEA50 NPs had the highest EE (~95%) and LE (>9 wt%), while NPs with lower or higher Phe/Arg ratios had lower EE and LE (Figures 2b and S5a). These findings support our hypothesis that both the cationic and hydrophobic characteristics of PEAs may be important for their interaction with proteins. Interestingly, all PLGA-PEA NPs exhibited similar EE of insulin (~90%). The EE and LE of the surface-loaded Tf are shown in Figures 2c and S5b. A similar trend was observed for PEA NPs and PLGA-PEA NPs, implying that the surface loading was mainly mediated by the interaction of PEAs with the Tf protein.

The release profiles of insulin from PEA and PLGA-PEA NPs are shown in Figures 2d–e. For PEA NPs, slower release was observed for NPs with higher Phe/Arg ratio (Figure 2d). Interestingly, the insulin release kinetics exhibited a completely opposite trend for PLGA-PEA NPs as compared to PEA NPs, with the release rate being slower for lower Phe/Arg ratio (Figure 2e). The cationic characteristic of the PEA might have dual effects in influencing the release of insulin. In PEA NPs, stronger cationic properties can cause less compactness of the NP structure, and thus increasing the diffusion rate of insulin. The positive charge may also slow the release rate due to attraction for the negatively charged insulin. As PLGA might increase the compactness of highly cationic NPs by increasing the hydrophobicity and diluting the charge density, the charge interaction between PEA and insulin could then become the dominant factor in controlling protein release from the PLGA-PEA NPs. The NPs also exhibited sustained release in simulated gastric fluid, simulated intestinal fluid and fluid of different pH at sequential order (Figures S6 a–c). In addition, we also investigated the release profile of the surface-loaded Tf from the NPs (Figure S6d and e). Tf was released most slowly from NPs with PEA50 (either PEA or PLGA-PEA NPs). Since the release of Tf does not involve diffusion through the NP matrix, the release rate may be mainly controlled by the protein interactions with the surface of NPs. Moreover, the enzymatic test with pancreatin showed that both insulin and Tf were well protected when loaded with the NPs (Figure S7).

Cellular internalization of Tf-coated NPs was compared with BSA-coated NPs using Caco-2 cells. The PLGA-PEA NPs were loaded with DiD fluorescent dye, which excited no detectable release (Figure S8). The uptake of Tf-coated NPs was ~ 5-fold higher than that of BSA-coated NPs (Figure 3a–b),suggesting the effectiveness of Tf in improving epithelial uptake of NPs. To examine internalization pathway, NPs were incubated with Caco-2 cells in presence of different specific inhibitors: 5-N-ethyl-N-isoproamiloride (EIPA), filipin, and chlorpromazine, for three pathways: macropinocytosis, and caveolae- and clathrin-mediated endocytosis, respectively[10]. The uptake was significantly reduced for BSA-coated NPs

only treated with EIPA, indicating a major role of macropinocytosis (Figure 3c). In comparison, the uptake of Tf-coated NPs was reduced by ~65% with chlorpromazine, inhibitor of clathrin-mediated endocytosis. For further validation, we co-incubated DiD-containing NPs with Alexa Fluor 488 (AF488)-labeled Tf or dextran, which are internalized by clathrin-mediated endocytosis and macropinocytosis, respectively. Tf-coated NPs were co-localized with AF488-Tf, whereas BSA-coated NPs were largely co-localized with the AF488-dextran (Figure S9). Therefore, the Tf enhanced the epithelial internalization of the NPs by changing the uptake pathway via the specific ligand-receptor interaction.

In vitro transepithelial activity of NPs was evaluated by measuring their transport from apical to basolateral side of Caco-2 cell monolayers on Transwell® permeable supports. 4-fold greater fluorescence intensity was observed for Tf-coated NPs relative to BSA-coated NPs (Figure 3d). Moreover, the amount of basolateral Tf-coated NPs was significantly reduced when co-incubated with free Tf as a competitive blocking agent, implying the role of Tf in the transport of NPs. Besides, the NP treatment did not affect the integrity of the cell monolayer (Figure S10), avoiding potential safety issues[5]. We then tested *in vivo* transport of Tf-coated NPs across intestinal epithelium of mouse. Figure 4a shows representative images of intestine sections. Impressively, for the Tf-coated NPs, fluorescence signals were observed in epithelium and basolateral side of epithelial cells, indicating the successfully transport of the NPs. Little signal of BSA-coated NPs was detected in the villi.

We examined bioactivity of insulin after the processes of NP preparation and drug release. Figure 4b indicated that the released insulin generated a hypoglycemic response analogous to an equivalent dose of free insulin solution after subcutaneous injection. Hypoglycemic response after oral administration of the Tf-coated NPs was then tested on normal rats. Four different formulations of Tf-coated NPs were tested (PEA50, PEA75, PLGA-PEA50, and PLGA-PEA75 NPs). The hypoglycemic effect generated by BSA-coated NPs was not significantly different from free insulin (Figure 4c). All four tested Tf-coated NPs elicited a significant hypoglycemic response, reducing glucose during the first 1–6 hours after administration(Table S3). It is worth noting that, despite the lasting of insulin release, the glucose levels in all these NP groups exhibited no significant difference relative to the control group at 8–10 hours post administration, which might be attributed to the systemic clearance of the NPs. In addition, the hypoglycemic effect was also tested on mice with insulin-dependent (type I) diabetes mellitus. BSA-coated NPs only led to a mild hypoglycemic response with no significant difference from the control. Tf-coated NPs elicited a remarkable hypoglycemic response at the dose of 50 U/kg (Table S4). It should be mentioned that small animals usually have a rapid gastric emptying rate, which could minimize the degradation of NPs and the installed protein ligands/therapeutics in harsh gastric conditions. The effectiveness of the NP platform in large animal species still needs further investigation. In summary, with a unique family of Phe- and Arg-based PEA polymers, we developed a novel NP platform capable of effectively installing protein ligands on the particle surface, while simultaneously carrying and delivering therapeutic proteins. The proteins could be released in a controlled manner with a range of release kinetics. Using Tf as a model targeting protein, we demonstrated that the surface-loaded protein could enhance their transepithelial transport via receptor-mediated transcytosis. *In vivo* work further revealed that the Tf-coated NPs could be transported across intestinal epithelium, and

resulted in a notable hypoglycemic response. However, more efforts will be needed to further study parameters that might influence the behavior and therapeutic efficacy of the NPs, such as the ideal release profile and the choice of polymer with optimal cationic/hydrophobic property. Meanwhile, for further applications, the NPs might need to be encapsulated in enteric capsules to improve efficiency by avoiding contact with gastric environment. We expect this work represents a proof of concept of a novel targeting strategy in which non-covalently coated proteins change the cellular and *in vivo* behaviors of the polymeric NPs.

Supplementary Material

Refer to Web version on PubMed Central for supplementary material.

Acknowledgments

This work was supported by the National Institutes of Health (NIH) grants (EB015419, R00CA160350, and CA151884), the Movember-Prostate Cancer Foundation (PCF) Challenge Award, the National Research Foundation of Korea K1A1A2048701, the David H. Koch-PCF Program in Cancer Nanotherapeutics, and the National Natural Science Foundation of China (81173010). O.C.F. has financial interest in BIND Therapeutics, Selecta Biosciences, and Blend Therapeutics.

References

1. (a) Leader B, Baca QJ, Golan DE. Nat. Rev. Drug Discov. 2008; 7:21–39. [PubMed: 18097458] b) Vermonden T, Censi R, Hennink WE. Chem. Rev. 2012; 112:2853–2888. [PubMed: 22360637]
2. Frokjaer S, Otzen DE. Nat. Rev. Drug Discov. 2005; 4:298–306. [PubMed: 15803194]
3. (a) Mo R, Jiang T, Di J, Tai W, Gu Z. Chem. Soc. Rev. 2014; 43:3595–3629. [PubMed: 24626293] b) Yu J, Zhang Y, Ye Y, DiSanto R, Sun W, Ranson D, Ligler FS, Buse JB, Gu Z. Proc Natl Acad Sci U S A. 2015; 112:8260–8265. [PubMed: 26100900]
4. Pridgen EM, Alexis F, Farokhzad OC. Clin Gastroenterol Hepatol. 2014; 12:1605–1610. [PubMed: 24981782]
5. Pridgen EM, Alexis F, Kuo TT, Levy-Nissenbaum E, Karnik R, Blumberg RS, Langer R, Farokhzad OC. Sci. Transl. Med. 2013; 5:213ra167.
6. Wu J, Kamaly N, Shi J, Zhao L, Xiao Z, Hollett G, John R, Ray S, Xu X, Zhang X, Kantoff PW, Farokhzad OC. Angew. Chem. Int. Ed. 2014; 53:8975–8979.
7. (a) Wiley DT, Webster P, Gale A, Davis ME. Proc Natl Acad Sci U S A. 2013; 110:8662–8667. [PubMed: 23650374] b) Zhu ZB, Makhija SK, Lu B, Wang M, Rivera AA, Preuss M, Zhou F, Siegal GP, Alvarez RD, Curiel DT. Virology. 2004; 325:116–128. [PubMed: 15231391] c) Kawabata H, Yang R, Hirama T, Vuong PT, Kawano S, Gombart AF, Koeffler HP. J Biol Chem. 1999; 274:20826–20832. [PubMed: 10409623]
8. Wu J, Chu C-C. J. Mater. Chem. B. 2013; 1:353–360.
9. Akagi T, Watanabe K, Kim H, Akashi M. Langmuir. 2010; 26:2406–2413. [PubMed: 20017513]
10. Zhang J, Zhu X, Jin Y, Shan W, Huang Y. Mol Pharm. 2014; 11:1520–1532. [PubMed: 24673570]

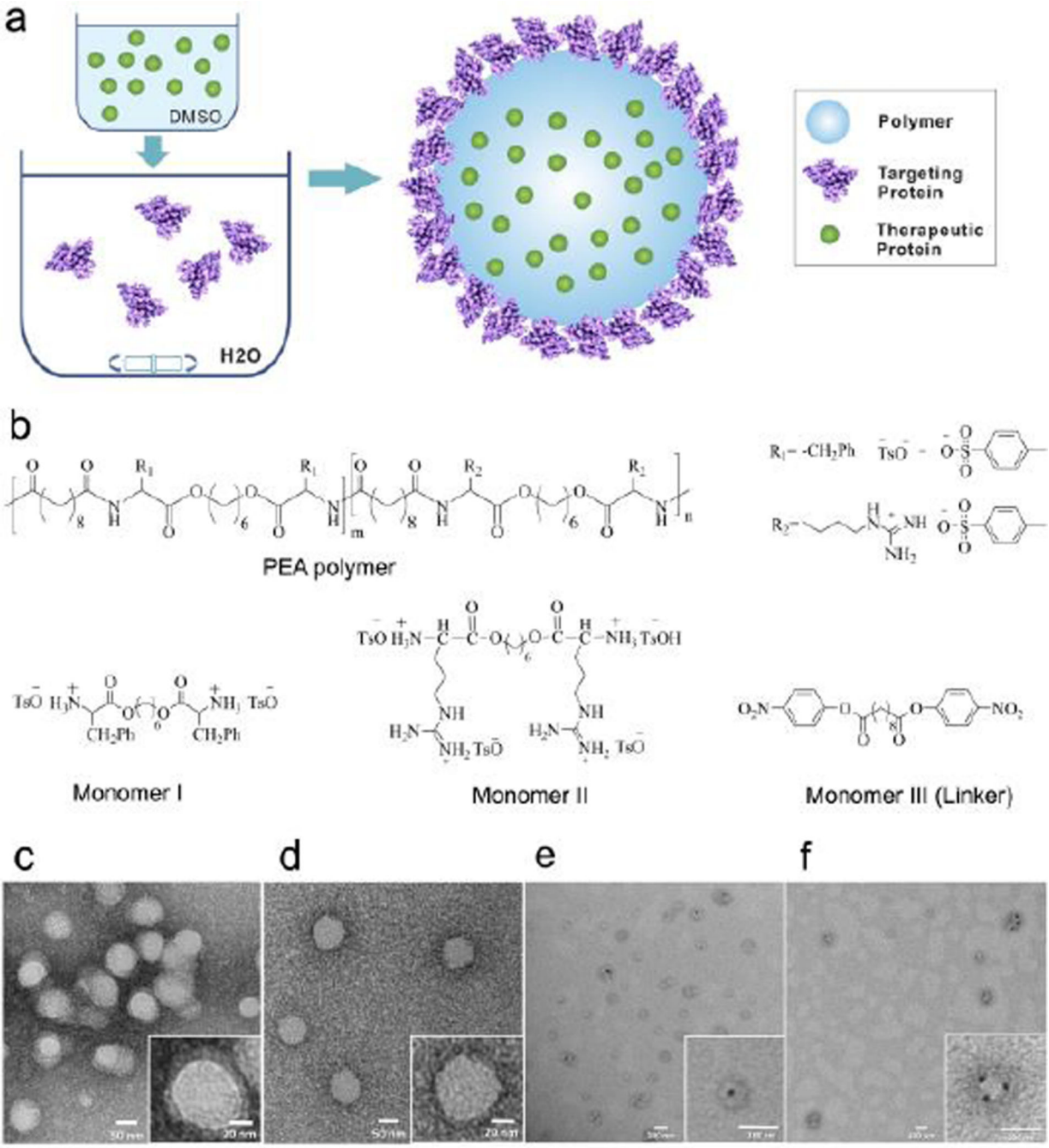

Figure 1.

(a) Schematic diagram of the NP structure and the self-assembly process for NP; (b) Chemical structures of monomers and the PEA polymer; TEM image of PEA75 NPs (c) with and (d) without surface proteins; TEM image of PEA75 NPs with (e) inner or (f) surface loaded BSA-Au.

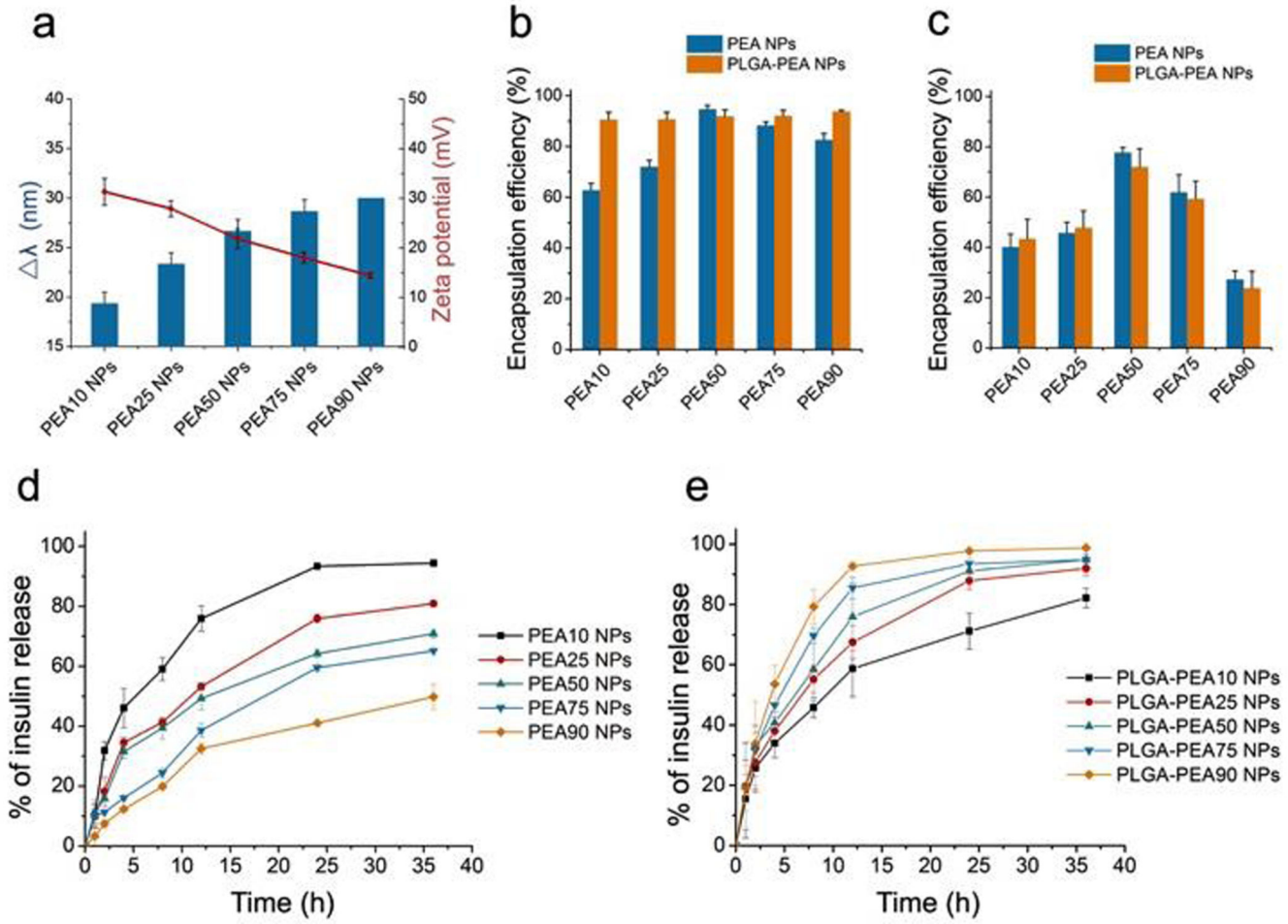

Figure 2.

(a) Zeta potential of different PEANPs and the peak wavelength shift of CBB (Δλ) incubated with different NPs; Encapsulation efficiency of (b) interiorly loaded insulin and (c) surface-loaded Tf for different NPs; Release profile of insulin from different (d) PEA NPs and (e) PLGA-PEA NPs.

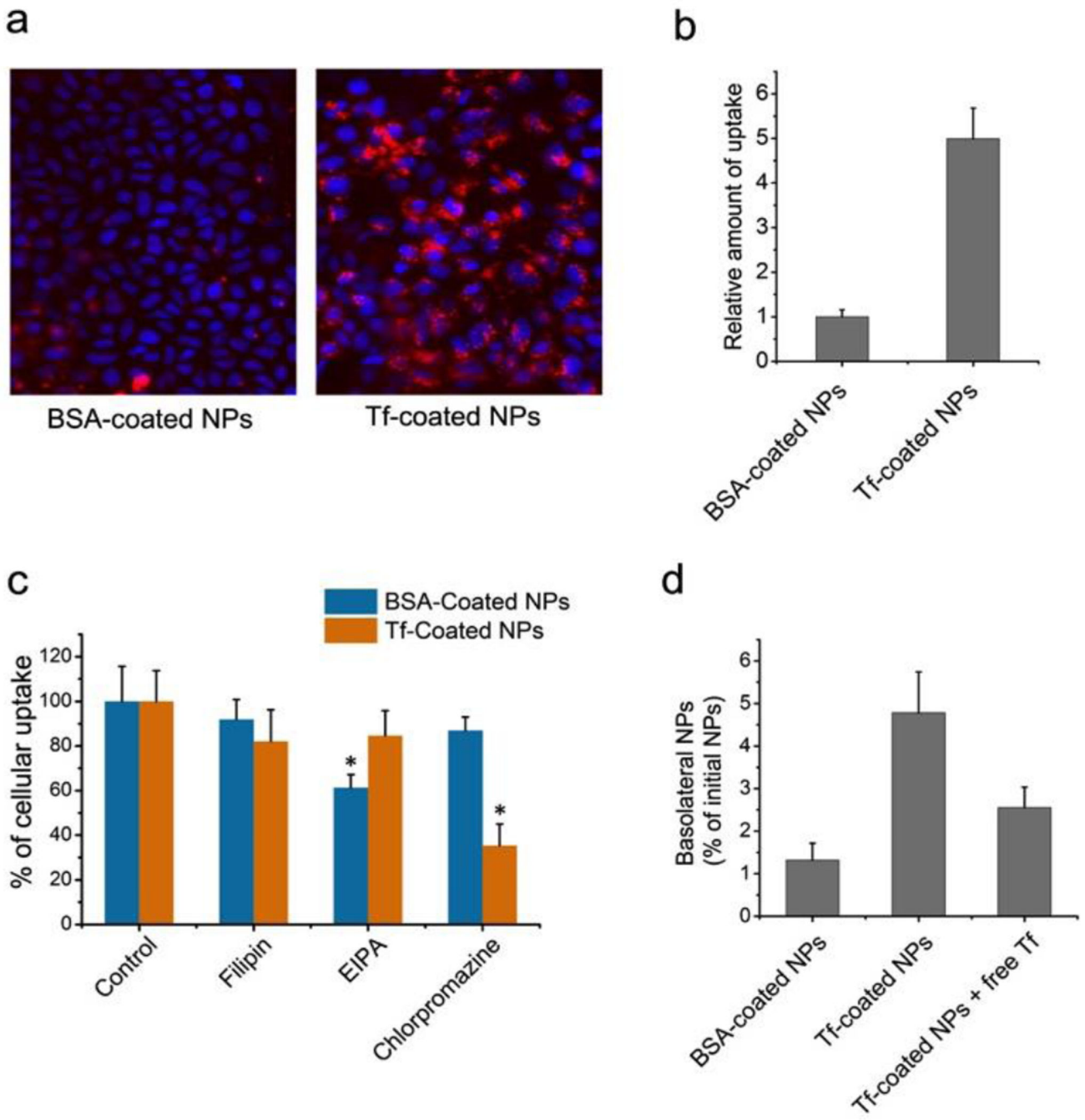

Figure 3.

(a) Fluorescence images of Caco-2 cells treated with BSA-coated vs. Tf-coated NPs labeled with fluorophore (red); (b) Quantitative analysis of the relative uptake of BSA- vs. Tf-coated NPs; (c) Relative inhibition of NP uptake with specific endocytotic inhibitors (* $p<0.05$ vs. control); (d) *In vitro* transepithelial transport of BSA- and Tf-coated NPs, and Tf-coated NPs with free Tf as a competitive blocking agent (n = 4 per group).

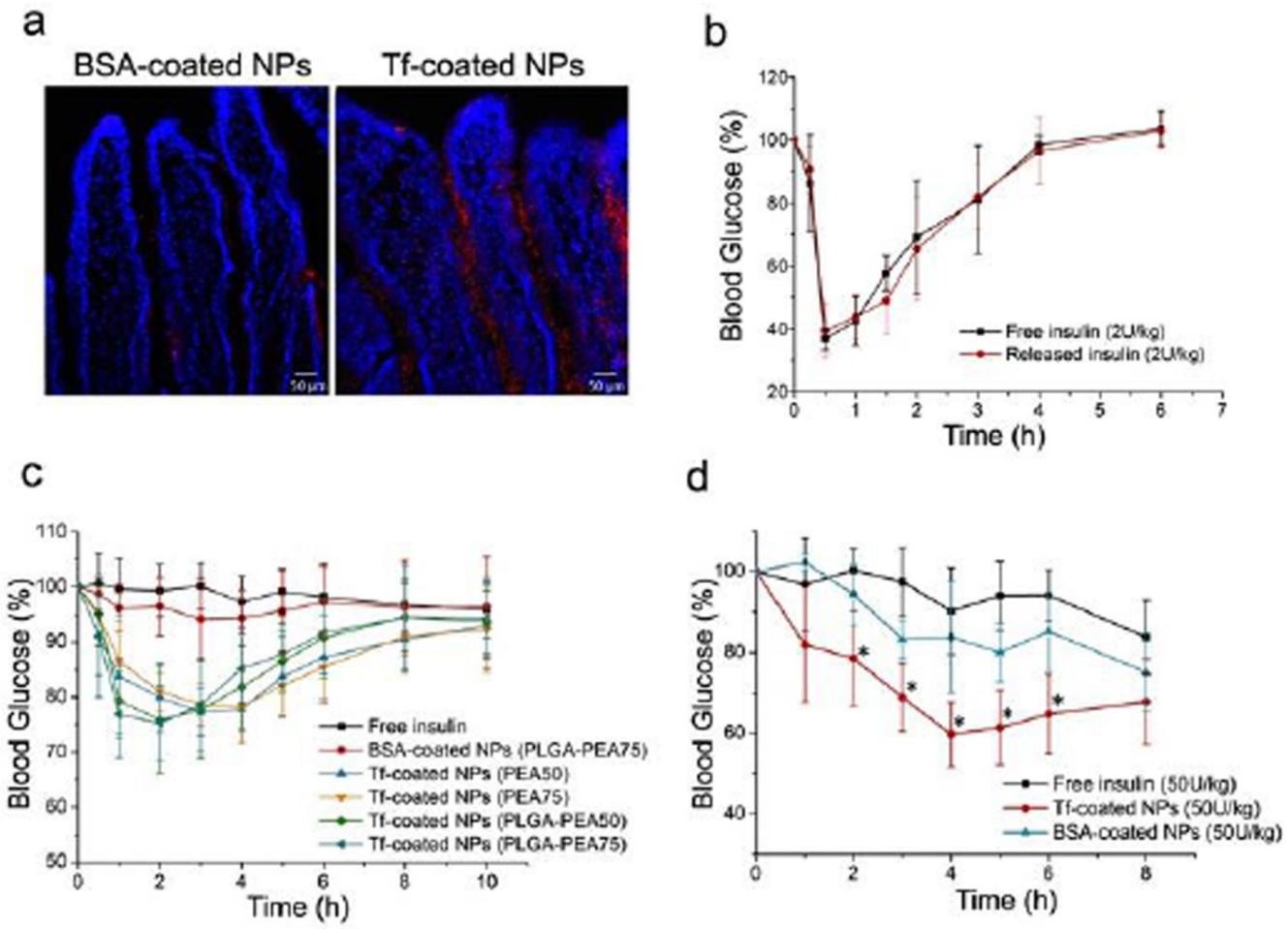

Figure 4.

(a) Fluorescence images of sections of mouse intestine after administration of BSA- or Tf-coated NPs (red). Cell nuclei were stained with DAPI (blue); (b) Blood glucose response of normal rats to free insulin or insulin released from the NPs (2 U/kg) (n = 4); (c) Blood glucose response of normal rats to free insulin solution, BSA-coated NPs, and Tf-coated NPs with different formulations following oral gavage (n = 6); (d) Blood glucose response of diabetic mice to free insulin solution, BSA-coated NPs, and Tf-coated NPs following oral administration (n = 6, * $p<0.05$ *vs.* free insulin).